SUPPLEMENTARY FIGURES

Dimitrova et al., Figure S1

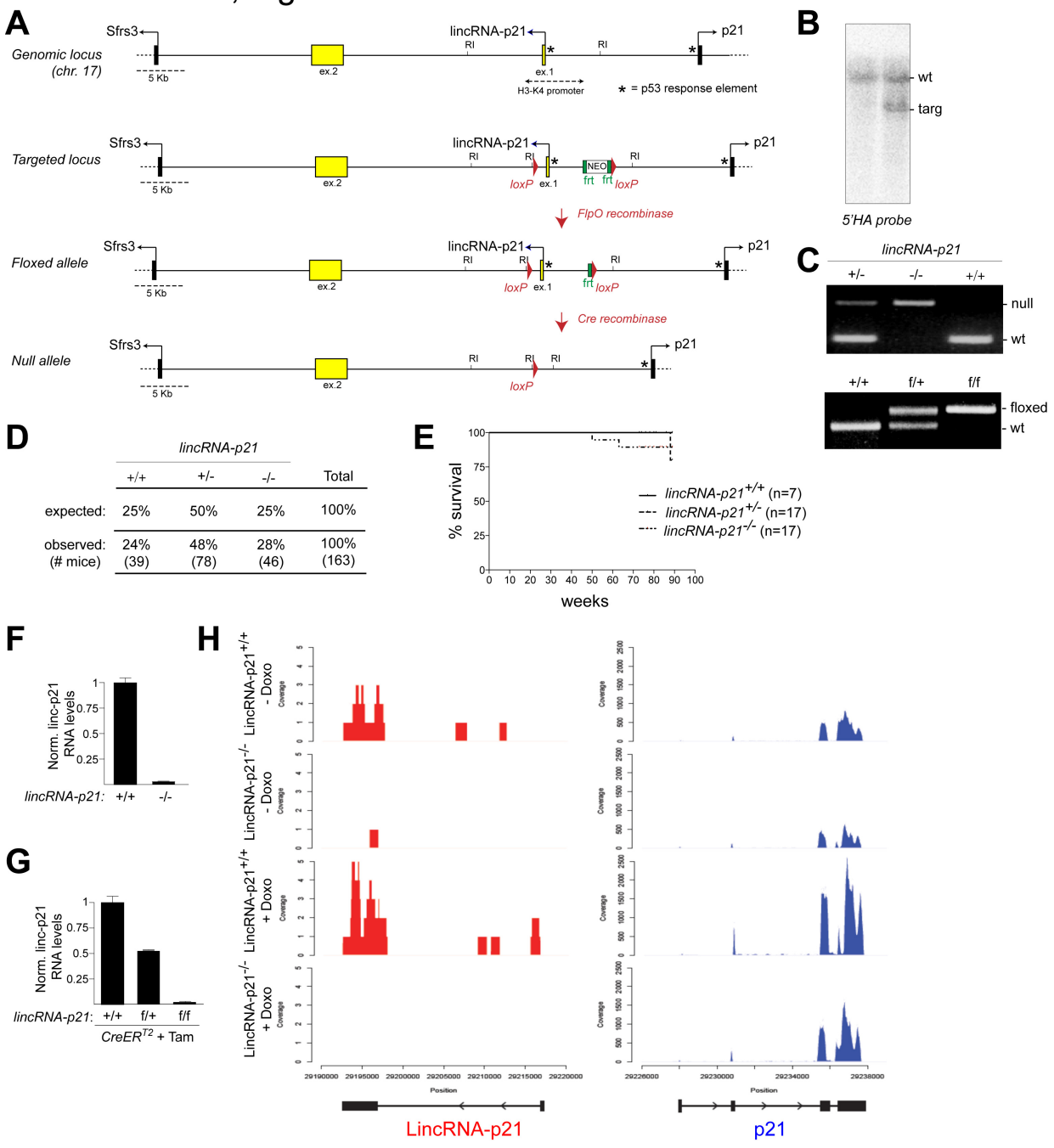

Figure S1. Generation of lincRNA-p21 conditional knockout mice and MEFs and initial characterization, related to Figure 1.

(A) Schematic of the targeting strategy and the generation of the indicated alleles. * indicate the p53REs in the promoters of p21 and lincRNA-p21.

(B) Southern blot verification of correct targeting using EcoRI digest and a probe complementary to a region outside of the 5' homology arm (HA).
(C) PCR genotyping of tails of mice with indicated genotypes
(D) Genotype distribution of pups from lincRNA-p21 heterozygous crosses. Expected numbers are based on Mendelian distribution.
(E) Survival curve of mice of indicated genotypes.
(F-G) qRT-PCR analysis of lincRNA-p21 levels in MEFs of indicated genotypes and treatments.
(H) Genome browser snapshot of the reads of lincRNA-p21 and p21 determined by RNA-seq analysis of RNA isolated from indicated cell lines and treatments.

Dimitrova et al., Figure S2

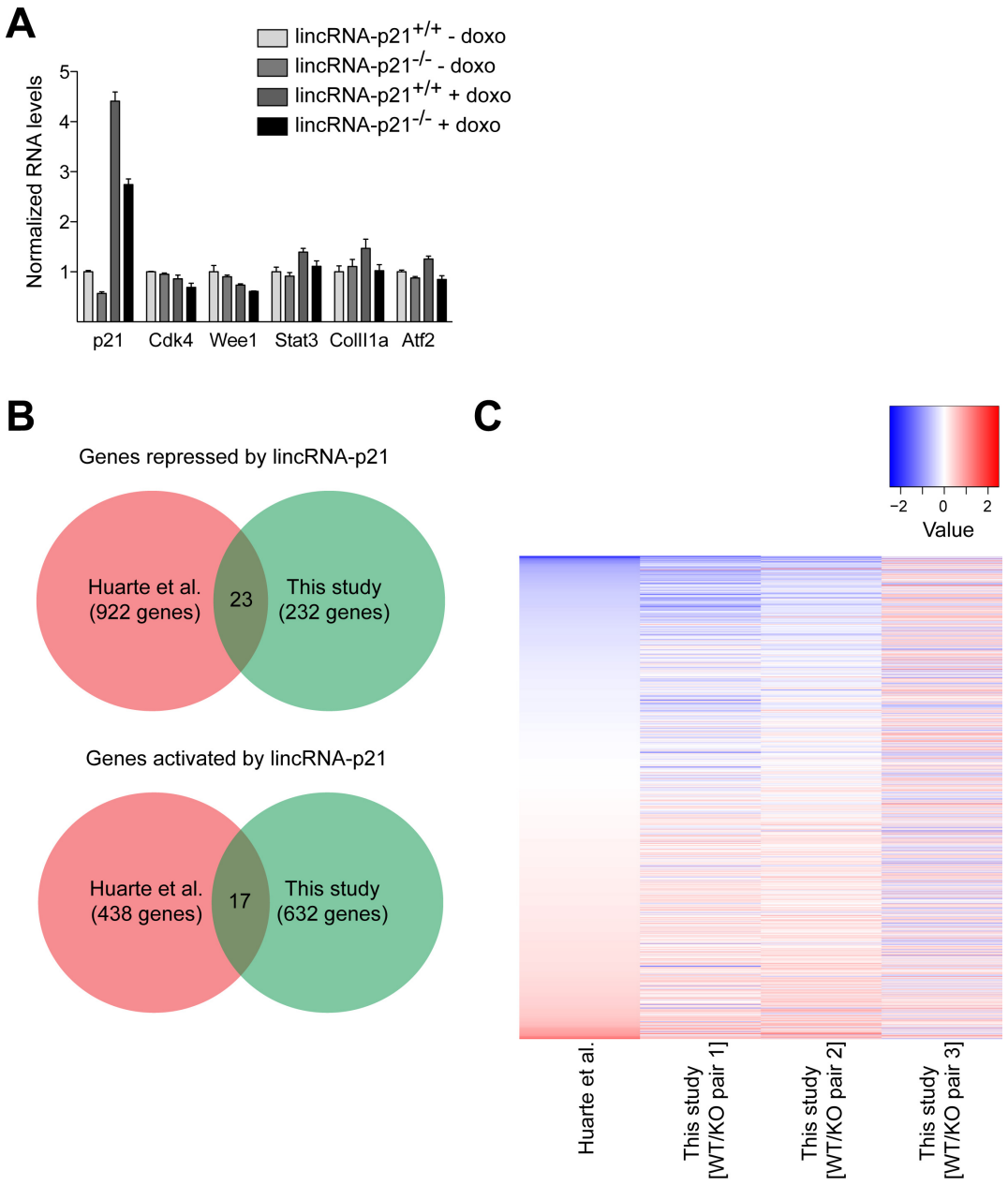

Figure S2. Comparison of lincRNA-p21-regulated gene sets between this study and a previously published study (Huarte et al., 2010), related to Figure 1.

(A) qRT-PCR analysis of p21 and five other genes previously proposed to be targets of lincRNA-p21-mediated repression.

(B) Venn diagrams of the overlap of lincRNA-p21-repressed and -activated genes as determined by the genetic approach in this study (Table S1) versus the Huarte et al.

2010 study, which utilized an RNAi-mediated approach to downregulate lincRNA-p21 levels.

(C) Heatmap comparison of the differentially expressed genes in the indicated lincRNA-p21-responsive gene sets (Huarte et al., 2010 study versus the three littermate pairs used in this study (Table S1)).

Dimitrova et al., Figure S3

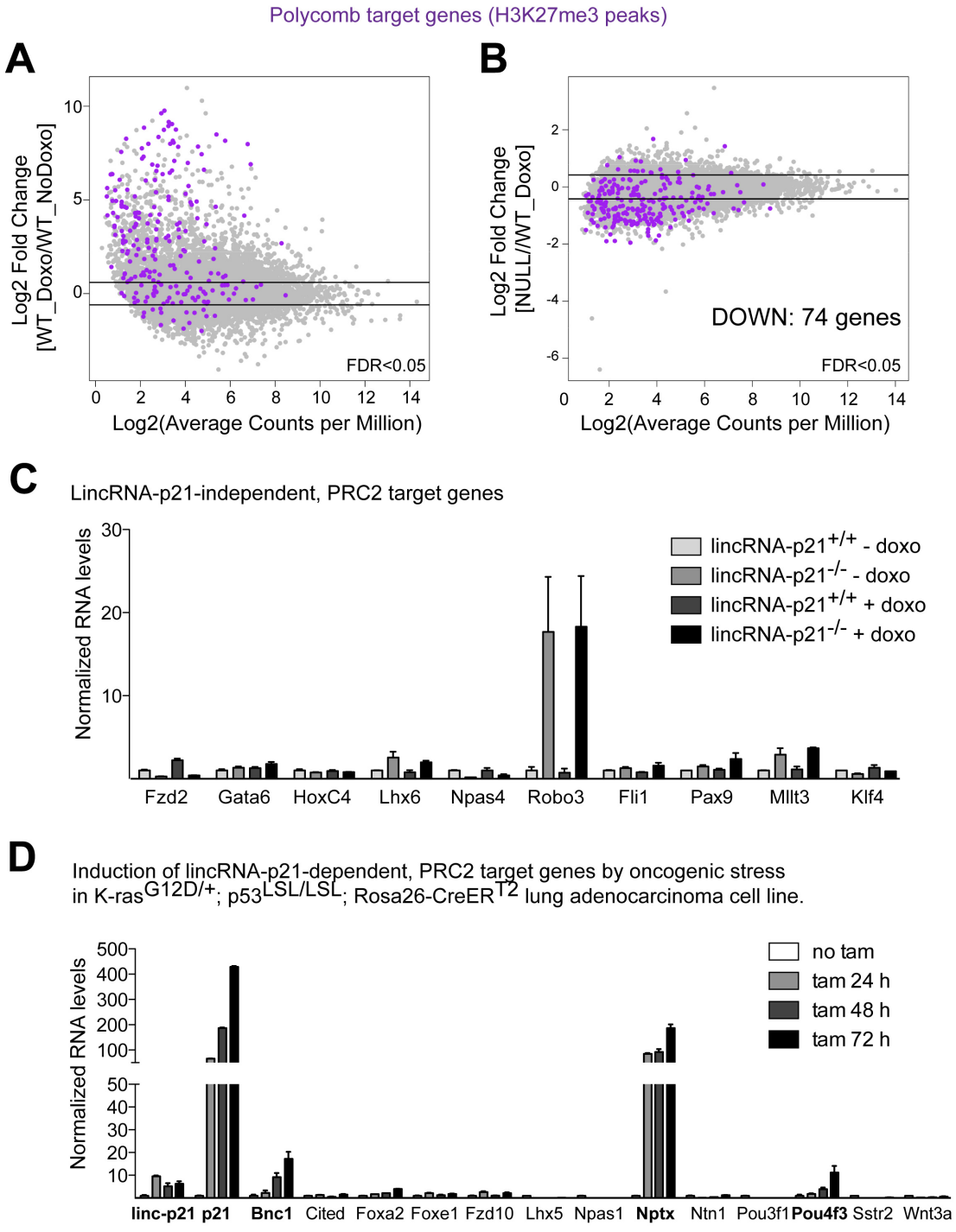

Figure S3. Characterization of the PRC2 targets gene set, related to Figure 2.

(A) Scatter plot of the doxorubicin-dependent gene set. Polycomb target genes (H3K27me3 peaks, see Table S3) are highlighted in purple. Data indicate that a significant fraction of these genes is induced in response to the doxorubicin treatment.

(B) Scatter plot of the lincRNA-p21-regulated gene set (Table S1). Polycomb target genes (H3K27me3 peaks, see Table S3) are highlighted in purple. The number of genes with reduced expression levels (DOWN) in doxorubicin-treated, lincRNA-p21-deficient MEFs compared to controls is indicated (Related to Table S3).

(C) qRT-PCR analysis of the expression levels of lincRNA-p21 non-responsive genes selected from the PRC2 targets gene set (MSigDB: Benporath_PRC2_Targets, see Table S3). Data indicate that lincRNA-p21 does not affect PCR2 genes globally. Cell lines and treatments as indicated.

(D) qRT-PCR analysis of the expression levels of lincRNA-p21-responsive, PRC2 target genes in RNA isolated from a $Kras^{G12D/+}$; $p53^{LSL/LSL}$; Rosa26-$CreER^{T2}$ lung cancer cell line, treated as indicated with tamoxifen to restore p53 expression.

Dimitrova et al., Figure S4

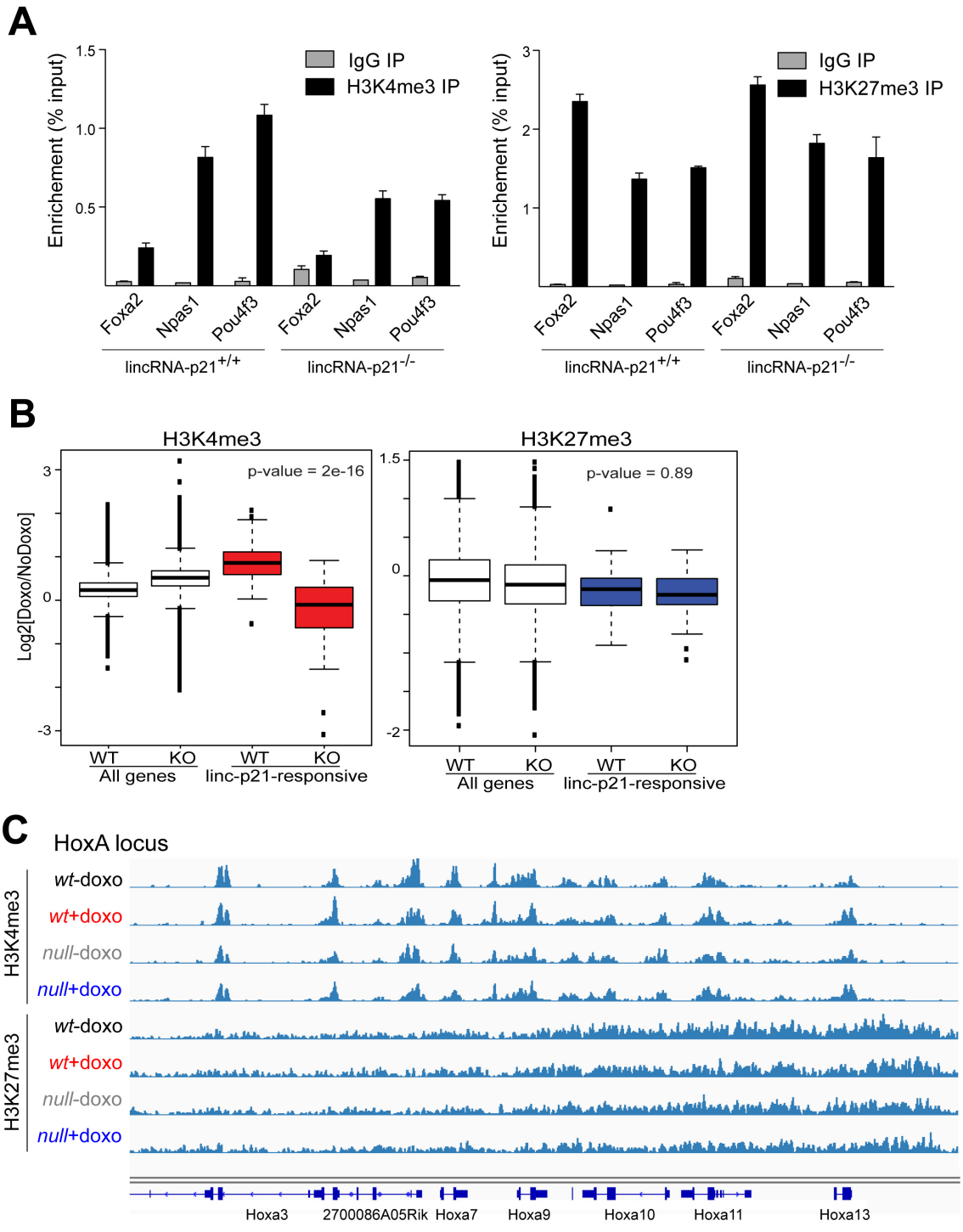

Figure S4. Effect of lincRNA-p21 deficiency on chromatin, related to Figure 2.

(A) ChIP-qPCR analysis of the enrichment of H3K4me3 *(left)* and H3K27me3 *(right)* at the promoters of the indicated lincRNA-p21-responsive, PRC2 target genes in doxorubicin-treated lincRNA-p21$^{+/+}$ and lincRNA-p21$^{-/-}$ MEFs. IgG immunoprecipitation was used as a negative control.

(B) Box plot analysis of the enrichment levels of H3K4me3 *(left)* and H3K27me3 *(right)* at all genes or at lincRNA-p21-responsive, Polycomb target genes (see Table S3) in doxorubicin-treated samples relative to untreated cells of indicated genotypes.

(C) Genome browser snapshot of the H3K4me3 and H3K27me3 ChIP-seq reads at the HoxA locus in lincRNA-p21$^{+/+}$ (wt) and lincRNA-p21$^{-/-}$ (null) MEFs, collected at 24 hours following mock or doxorubicin treatment.

Dimitrova et al., Figure S5

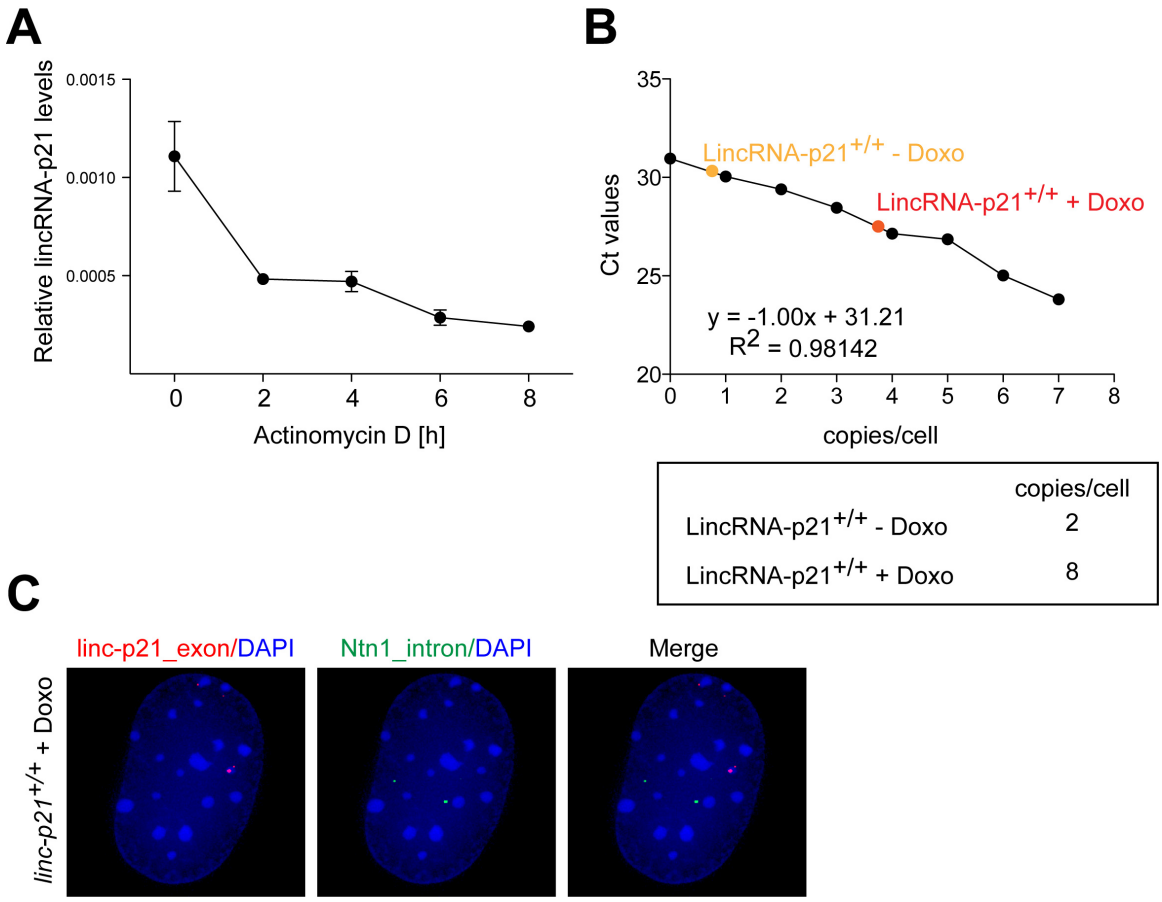

Figure S5. Determination of lincRNA-p21 half-life and copy number, related to Figure 3.

(A) qRT-PCR analysis of lincRNA-p21 RNA levels in doxorubicin-treated, wild-type MEFs harvested at indicated time-points following treatment with 5 mg/ml Actinomycin D.

(B) Calculation of lincRNA-p21 copy number. Standard curve of Ct values was performed by qPCR using a dilution series of lincRNA-p21 DNA template of known concentration, corresponding to the region amplified during qRT-PCR. Next, qPCR analysis of lincRNA-p21 was performed with cDNA generated from RNA isolated from a known number of lincRNA-p21-proficient cells, untreated or treated with doxorubicin. The Ct values were fitted on the standard curve and used to calculate the number of lincRNA-p21 molecules per cell (multiplied by 2 to account for the fact that cDNA is single stranded, whereas the DNA template used to generate the standard curve is double-stranded).

(C) LincRNA-p21 RNA does not localize at the Ntn1 locus. LincRNA-p21 RNA was detected using probes specific to the exon of lincRNA-p21 and the Ntn1 locus was detected by intron-specific Ntn1 probes using single molecule RNA FISH. DNA was counterstained with DAPI.

* Note: The analysis was limited to Ntn1 because the majority of PRC2 target genes lack introns or contain very short introns, which were not amenable to detection by single molecule RNA FISH.

Dimitrova et al., Figure S6

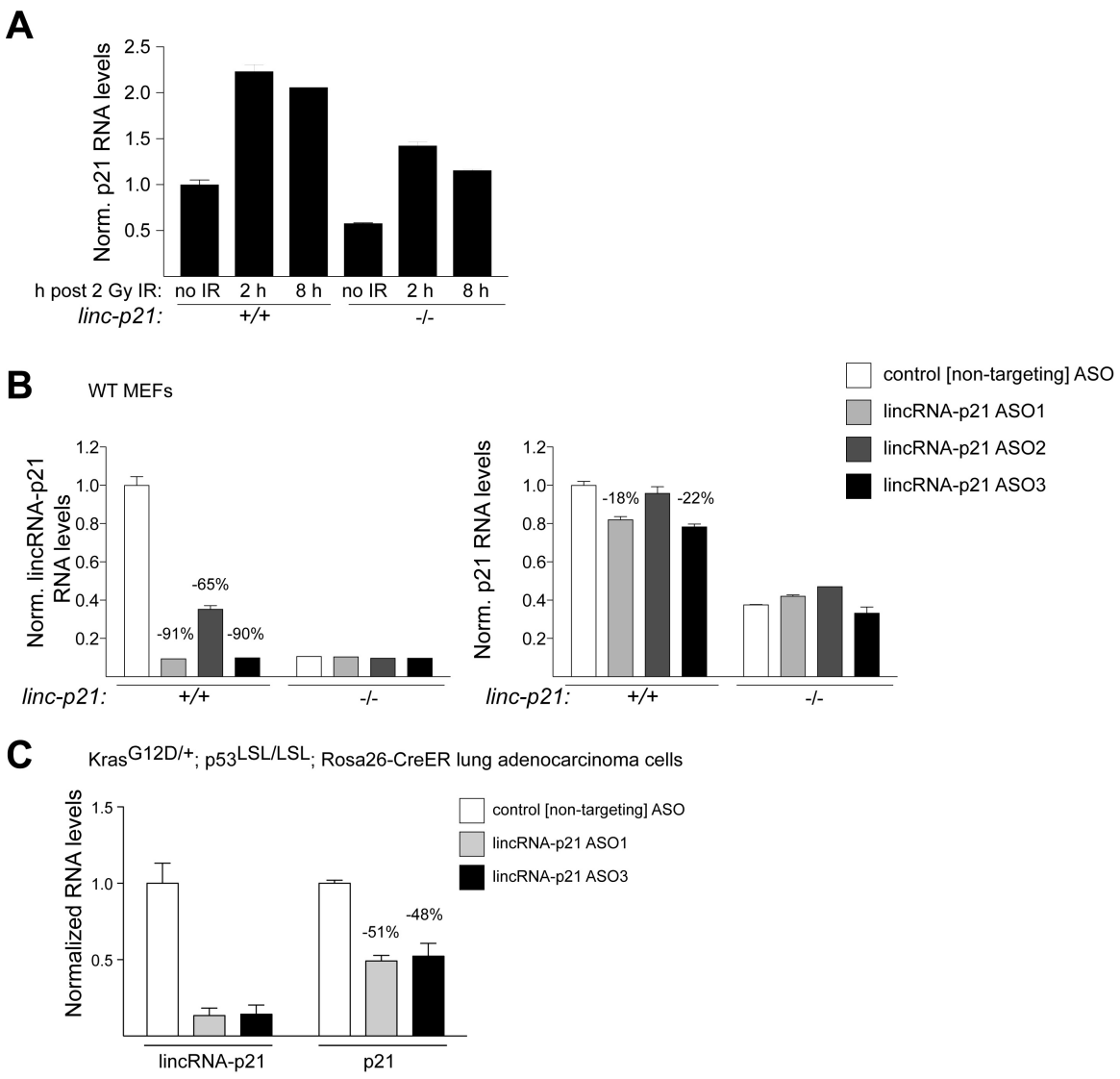

Figure S6. LincRNA-p21 positively regulates p21 levels, related to Figure 4.

(A) qRT-PCR analysis of p21 RNA levels in MEFs of indicated genotypes harvested at indicated time-points following 2 Gy irradiation. p21 was still induced with the same kinetics in cells lacking lincRNA-p21 but its levels were reproducibly reduced.

(B) qRT-PCR analysis of lincRNA-p21 *(left)* and p21 *(right)* RNA levels in MEFs of indicated genotypes transfected twice, at a 48-hour interval, with the indicated ASOs and harvested 96 hours after the first transfection. LincRNA-p21-specific ASO1 and ASO3

reproducibly led to greater than 90% knockdown and affected p21 levels, whereas ASO2 did not produce an efficient knockdown and did not affect p21 levels.

(C) qRT-PCR analysis of lincRNA-p21 and p21 expression levels in RNA isolated from a $Kras^{G12D/+}$; $p53^{LSL/LSL}$; $Rosa26\text{-}CreER^{T2}$ lung cancer cell line, 24 h post transfection with indicated control (non-targeting) or two independent lincRNA-p21-specific ASOs and concomitant treatment with tamoxifen to restore p53 expression.

Dimitrova et al., Figure S7

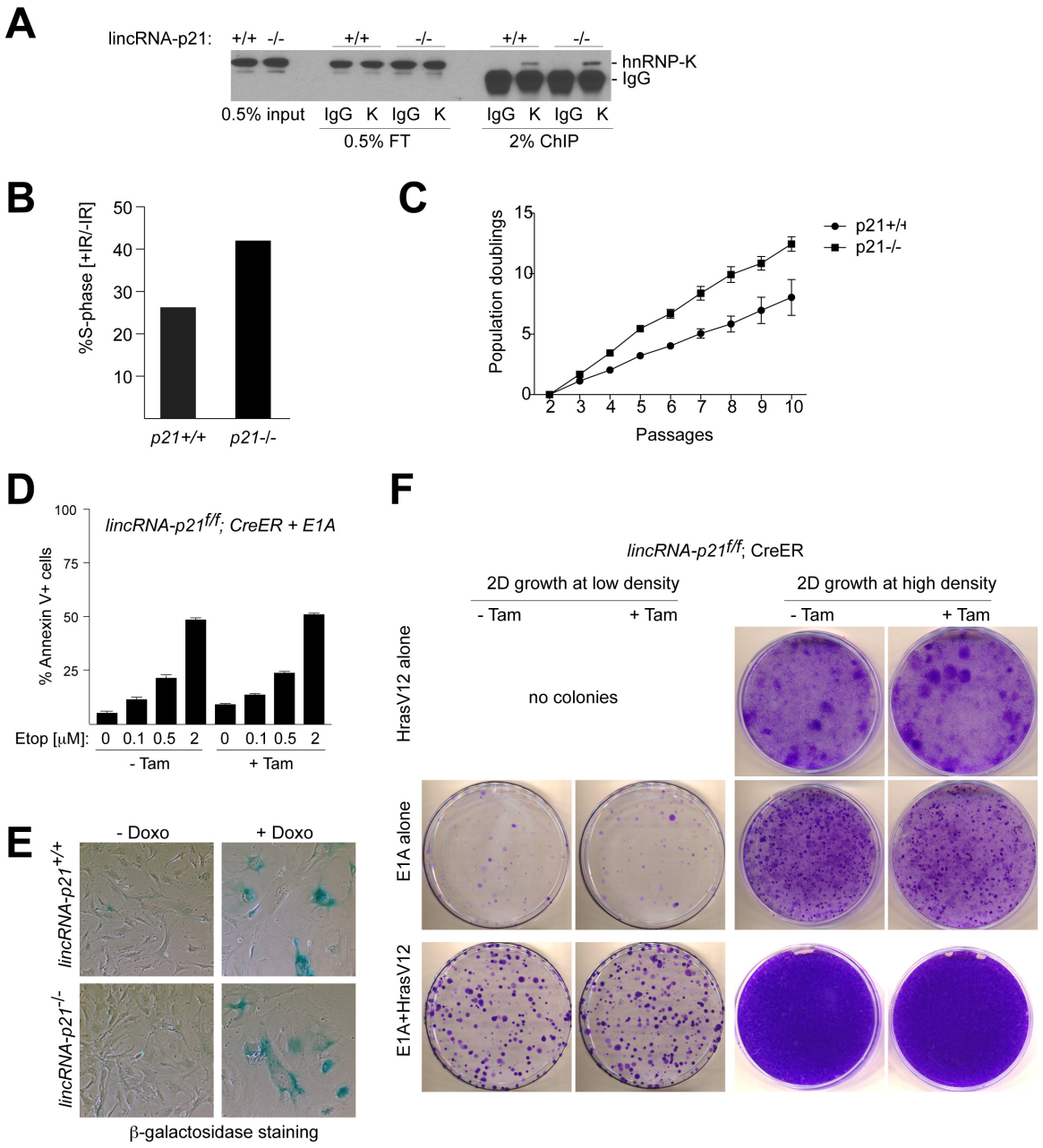

Figure S7. Related to Figures 6 and 7.

(A) Efficiency of hnRNP-K ChIP. Immunoblot detection of hnRNP-K in indicated fraction of input, flow-through (FT) and hnRNP-K- or control IgG-immunoprecipitated chromatin (ChIP), indicating that hnRNP-K immunoprecipitation was specific but of low efficiency.

(B-C) Effect of p21 deficiency on the G1/S checkpoint and proliferation rates.

(B) FACS analysis of the fraction of BrdU-positive cells in irradiated samples relative to untreated cells. Data are representative of two independent experiments.

(C) Proliferation of $p21^{+/+}$ and $^{-/-}$ MEFs isolated from littermate embryos. Data are representative of three independent experiments.

(D-F). LincRNA-p21 loss does not affect apoptosis, senescence, or cellular transformation.

(D) FACS analysis of Annexin V-positive cells in samples collected from lincRNA-$p21^{f/f}$; $CreER^{T2}$ MEFs infected with retroviral E1A, harvested at 7 days following mock treatment or tamoxifen-mediated depletion of lincRNA-p21 and 24 hours following treatment with the indicated doses of etoposide (Etop) (Lowe et al., 1994).

(E) β-galactosidase staining of indicated MEFs analyzed at 7 days following mock or doxorubicin (Doxo) treatment.

(F) LincRNA-$p21^{f/f}$; CreER MEFs were infected with HrasV12 alone, E1A alone, or HrasV12+E1A via retroviral infections and treated with or without tamoxifen (Tam) prior to plating at low *(left)* or high *(right)* density in triplicates to evaluate colony-forming potential. No significant differences were observed between wild-type and lincRNA-p21-deficient cells.

LEGEND TO SUPPLEMENTARY TABLES

Table S1. Gene Expression Analysis, Related to Figures 1A and S2.
Lists of high-confidence, differentially expressed genes (upregulated or downregulated) following mock treatment or treatment with 0.5 μM doxorubicin for 24 hours in lincRNA-p21-deficient MEFs relative to littermate, wild-type controls (FDR<0.05, |Log 2 Fold Change|>0.43, n=3).

Table S2. GSEA, Related to Figure 1C. List of Molecular Signature Database (MSigDB) categories enriched for the differentially expressed genes (upregulated and downregulated genes are combined) from Table S1. Pathways identified in untreated *(Sheet 1)* or doxorubicin-treated *(Sheet 2)* samples are presented separately.

Table S3. PRC2 Target Genes, Related to Figure S3 and S4. PRC2 target genes were defined by (1) enrichment for the H3K27me3 chromatin mark (based on ChIP-seq performed in this study) or (2) the Benporath_PRC2_Tatgets MSigDB category. The set of incRNA-p21-responsive, PRC2 target genes were determined by overlapping these categories with the list of lincRNA-p21-regulated genes from Table S1.

Table S4. Primers, ASOs, and RNA FISH Probes Used in This Study, Related to Figures 2-7 and S1-S6. *(Sheet 1)* Sequence information about the primers used in qRT-PCR and ChIP-qPCR analyses; *(Sheet 2)* Sequence information about the lincRNA-p21-specific and control, non-targeting ASOs used in this study; *(Sheet 3)* Sequence information about the exon- and intron-specific probes used in RNA FISH analyses.

EXTENDED EXPERIMENTAL PROCEDURES

Mouse strains, cell culture, and drug treatments

The targeting construct for lincRNA-p21 was generated by conventional subcloning using appropriate restriction enzymes. In short, in order to prevent transcription initiation of lincRNA-p21, LoxP sites were placed on the flanks of the promoter region and the first exon of lincRNA-p21. An FRT-flanked neomycin-resistance cassette was placed for selection purposes downstream of exon 1. The lincRNA-p21 targeting construct was electroporated into hybrid 129/B6 F1 ES cells (V6.5). Correctly targeted clones were identified by Southern blotting using probes external to the targeting region. Two clones that had undergone successful homologous recombination were used to generate lincRNA-p21$^{targ/+}$ mice by tetraploid complementation. To reduce the risk of interfering with transcription, founders with the targeted allele were crossed to Flpe-deletor mice (*Actin-Flpe*) (Rodriguez et al., 2000) in order to remove the neomycin selection cassette and to generate the floxed allele, or bred to a Cre-deletor strain (*Actin-Cre*) (Lewandoski et al., 1997) to generate the lincRNA-p21 null allele. Successful recombination was verified by PCR. Primers and protocols for genotyping PCR are available upon request.

MEFs from littermate E13.5 embryos were obtained from timed crosses between lincRNA-p21$^{f/+}$; Rosa26-CreER^{T2} mice to generate lincRNA-p21$^{f/f,\ f/+}$ and $^{+/+}$; Rosa26-CreER^{T2} genotypes; between lincRNA-p21$^{+/-}$ mice to obtain lincRNA-p21$^{-/-}$ and $^{+/+}$ genotypes; between p21$^{+/-}$ mice to generate p21$^{+/+}$ and p21$^{-/-}$ MEF lines, and between lincRNA-p21$^{f/+}$ and p21$^{-/-}$ mice to generate lincRNA-p21$^{f/+}$; p21$^{+/-}$ and lincRNA-p21$^{f/+}$; p21$^{+/+}$ genotypes. MEFs were maintained as primary cultures in DMEM supplemented with 15% FBS, pen/strep, L-glutamine, non-essential amino acids, and β-mercaptoethanol. All experiments were performed with early passage MEFs, isolated from littermate embryos.

Viral infections

Lentivirus was produced in 293 cells by co-transfecting the TRE-lincRNA-p21 pSLIK or pLKO shRNA constructs with Δ8.2 and VSVG packaging constructs. The lentiviral constructs were introduced into lincRNA-p21$^{+/+}$ and $^{-/-}$ cells by 2 consecutive lentiviral infections, delivered at 24 hour-intervals, with virus-containing supernatant supplemented with 4 μg/ml polybrene. Following infections, 50 μg/ml hygromycin or 2 μg/ml puromycin selection was applied. To induce lincRNA-p21 expression, cells were

treated with 1 μg/ml doxycycline for 48 hours. Knockdowns of p21 and hnRNP-K were assayed by qRT-PCR. Only sh#4 led to a reproducible, greater than 90% knockdown of hnRNP-K. Infection with the pLKO vector expressing a luciferase-specific hairpin was used as a negative control.

E1A pLPC puro, Hras-V12 pWzl hygro, and c-myc pBabe puro retroviral constructs were introduced into lincRNA-p21$^{+/+}$ and $^{-/-}$ cells by 4 consecutive retroviral infections delivered at 12 hour-intervals with virus-containing supernatants from Phoenix cells, supplemented with 4 μg/ml polybrene. Puromycin (2 μg/ml) or hygromycin (50 μg/ml) selection was applied, as appropriate. For transformation assays, infection with the empty vector was used as a negative control.

Apoptosis, senescence, and G1/S checkpoint assays

The induction of apoptosis was monitored with the Guava Nexin Annexin V Binding Assay (EMD Millipore) and analyzed on a Guava EasyCyte Flow Cytometer (EMD Millipore) following treatment with 0.1, 0.5 or 2 μM etoposide for 24 hours.

To assay for senescence, MEFs were treated with 500 nM doxorubicin for 24 hours, washed with PBS once and cultured for 1 week under standard conditions. Cells were fixed in 0.5% glutaraldehyde diluted in PBS for 15 min at RT, washed 3 times in 1 mM $MgCl_2$ in PBS (not pH adjusted) and once in 1 mM $MgCl_2$ in PBS (pH 5.5). Cells were stained in β-gal Staining Solution (5 mM potassium ferrocyanide, 5 mM potassium ferricyanide, 1 mg/ml X-gal, 1 mM $MgCl_2$ in PBS, pH 5.5) for 6 hours at 37^{0}C. Cells were rinsed in PBS prior to imaging.

For the G1/S checkpoint assay, low passage MEFs were plated 24 hours prior to irradiation with 5.5 Gy. 16 hours following irradiation, cells were incubated with 10 μM BrdU for 4 hours. Cells were harvested by trypsinization, washed once in cold PBS, fixed in 70% EtOH, and analyzed for BrdU incorporation by FACS. Briefly, DNA was denatured for 30 min at RT in 2N HCl, 0.5% Triton-X100 and neutralized in 0.1M $Na_2B_4O_7$•$10H_2O$, pH 8.5. Cells were washed in Blocking buffer (0.5% BSA in PBS) and stained with anti-BrdU antibody conjugated to Alexa Fluor 488 (clone MoBU-1, B35130, Life Technologies) diluted in Blocking buffer for 30 min at RT in the dark. Cells were washed once in Blocking buffer, resuspended in Blocking buffer supplemented with 5 μg/ml propidium iodide and 0.1 mg/ml RNaseA, and analyzed on a Guava EasyCyte Flow Cytometer (EMD Millipore). The data represent the fraction of BrdU-positive cells in irradiated samples relative to non-irradiated samples for each cell line.

Reprogramming of primary MEFs

Early passage, primary lincRNA-p21-proficient and -deficient MEFs were infected with a cocktail of TetO-FUW-Oct4-2A-Sox2-2A-Klf4-2A-Myc- and M2-rtTA-expressing lentiviruses and plated for 6 days in primary MEF media supplemented with 2 μg/ml doxycycline and LIF (Esgro) (Carey et al., 2009). Alkaline phosphatase assay was performed using the Vector Red Alkaline Phosphatase Substrate Kit (Vector Labs, SK-51000). Briefly, cells were fixed for 2 min in 2% paraformaldehyde, rinsed in TBST (20 mM Tris-HCl, pH 7.4, 150 mM NaCl, 0.05% Tween 20) and stained for 30 min at RT in the dark. Cells were washed once in TBST prior to imaging by brightfield microscopy.

Single molecule RNA-Fluorescence *in situ* hybridization (RNA-FISH)

The sequences of 48 TMR-conjugated FISH probes specific to the exons of lincRNA-p21 RNA and 48 Quasar670-conjugated Stellaris FISH probes specific to the introns of lincRNA-p21 and Ntn1 are listed in Table S4. Single molecule RNA FISH was performed as previously described (Raj et al., 2008). Briefly, cells were grown on coverslips and fixed for 10 min in 3.7% formaldehyde at RT, followed by PBS washes. Cells were dehydrated overnight at 4^0C in 70% EtOH (diluted in DEPC-H_2O) and stored in 70% EtOH for up to a week at 4^0C. Coverslips were transferred to a hybridization chamber and equilibrated for 5 min in Wash solution (2xSSC, 10% formamide in DEPC-H_2O). Cells were incubated overnight at 30^0C with the indicated probes diluted in Hybridization solution (100 mg/ml dextran sulfate, 1 mg/ml *E.coli* tRNA, 0.2 mg/ml BSA, 2 mM vanadyl ribonucleoside complex, 2xSSC, 10% formamide, DEPC-H_2O). The next day, cells were washed 2 times for 30 min at 30^0C in Wash solution and mounted in antifade reagent (Vectashield Mounting medium with DAPI, Vector Laboratories). Images were captured using a DeltaVision RT microscope system (Applied Precision) with a PlanApo 60x 1.40 n.a. objective lens (Olympus America, Inc.). 5 μm Z-stacks at 0.5 μm were acquired using SoftWoRx software. Images were deconvolved and projected in two dimensions using SoftWoRx software.

Chromatin immunoprecipitation (ChIP)

Cells for each genotype and treatment were harvested by trypsinization, counted, washed once in PBS and cross-linked in 1% formaldehyde diluted in PBS for 10 min at RT. The reaction was stopped by adding glycine to a final concentration of 100 mM and

placing the samples on ice for 5 min. Cells were washed twice in cold PBS and the pellet was frozen and stored at -80^{0}C.

For p53, H3K4me3, and H3K27me3 ChIP, 5-10x10^6 nuclei were isolated by incubating the thawed cell pellet in Cell lysis buffer (20 mM Tris-HCl, pH 8.0, 85 mM KCl, 0.5% NP-40) supplemented with protease inhibitors (1 mM PMSF and Mini Complete Protease Inhibitor Cocktail Tablet (Roche)) on ice for 10 min. After centrifugation, the supernatant was removed and the nuclei were resuspended in Nuclei lysis buffer (50 mM Tris-HCl, pH 8.0, 10 mM EDTA, 1% SDS supplemented with protease inhibitors) and incubated for 10 min on ice. Next, chromatin was sonicated to 300-500 bp fragment size in an ice-water slurry for 2x10 min cycles using a Bioruptor sonicator (Diagenode). Sonicated lysates were centrifuged at maximum speed for 20 min and diluted in ChIP dilution buffer (0.01% SDS, 1.1% Triton-X100, 1.1 mM EDTA, 20 mM Tris-HCl, pH 8.0, 167 mM NaCl, supplemented with protease inhibitors). Input aliquots were saved at this point. The sonicated chromatin was used to set up chromatin immunoprecipitations with a p53 antibody or control IgG overnight at 4^{0}C on a rotator. Beads (PureProteome Protein G Magnetic Beads, Millipore) were blocked overnight in 1% BSA in PBS supplemented with 20 μg salmon sperm DNA (Invitrogen) per IP. The next day, the blocked beads were added to the immunoprecipitation reactions and samples were incubated on the rotator for an additional hour. Beads were washed once in each of the following washes for 5 min at 4^{0}C on the rotator: Low salt wash (0.1% SDS, 1% Triton-X100, 2 mM EDTA, 20 mM Tris-HCl pH8.0, 150 mM NaCl supplemented with protease inhibitors), High salt wash (0.1% SDS, 1% Triton-X100, 2 mM EDTA, 20 mM Tris-HCl, pH 8.0, 500 mM NaCl), LiCl wash (0.25 M LiCl, 1% NP-40, 1% Na deoxycholate, 1 mM EDTA, 20 mM Tris-HCl, pH 8.), and TE wash (10 mM Tris-HCl, pH 8.0, 1 mM EDTA).

hnRNP-K ChIP protocol was adapted from (Kagey et al., 2010). Briefly, thawed pellets from 1-2x10^7 cells were resuspended in LB1 (50 mM Hepes-KOH, pH 7.5, 140 mM NaCl, 1 mM EDTA, 10% glycerol, 0.5% NP-40, 0.25% Triton-X100, supplemented with protease inhibitors) and rotated end over end for 10 min at 4^{0}C. After centrifugation, the nuclei pellet was resuspended in LB2 (10 mM Tris-HCl, pH 8.0, 200 mM NaCl, 1 mM EDTA, 0.5 mM EGTA, supplemented with protease inhibitors) and incubated on a rotator for 10 min at 4^{0}C. Next, nuclei were pelleted, resuspended in Sonication buffer (50 mM HEPES-KOH, pH 7.5, 140 mM NaCl, 1 mM EDTA, 1 mM EGTA, 1% Triton-X100, 0.1% SDS, supplemented with protease inhibitors), and the chromatin was sheared to 300-500 bp fragments size in an ice-water slurry for 6x10 min cycles using a Bioruptor

sonicator (Diagenode). The sonicated lysate was centrifuged at maximum speed for 20 min to remove debris, an aliquot was reserved as input, and the supernatant was used to set up chromatin immunoprecipitations with beads pre-conjugated to an hnRNP-K antibody or control IgG. 20 μg of Salmon sperm DNA (Invitrogen) was added to each reaction to block non-specific binding. After overnight incubation at 4^0C on a rotator, the beads were washed twice in Sonication buffer, once in High salt sonication buffer (500 mM NaCl), once in LiCl wash, and once in TE wash.

For both protocols, after completely removing any remaining liquid from the washes, beads were resuspended in Elution buffer (50 mM Tris-HCl, pH 8.0, 10 mM EDTA, pH 8.0, 1% SDS) and incubated at 65^0C for 15 min with frequent vortexing to prevent settling of beads. After elution, the beads were pelleted and the supernatant was transferred to a new tube and incubated overnight at 65^0C to reverse the cross-linking. The next day, samples were treated with RNaseA for 2 hours at 37^0C, followed by a proteinase K treatment for 30 min at 55^0C. The DNA was purified by phenol-chloroform extraction and EtOH precipitation. The DNA pellet was air dried, resuspended in 200 μL H_2O.

RNA-seq and ChIP-seq analyses

RNA was isolated with the RNeasy Midi Kit (Qiagen). RNA-seq reads were mapped to the Ensembl NCBIM37 genome assembly using Tophat (ver 2.0.6) (Trapnell et al., 2009). The read counts at each Ensembl annotated gene were calculated with htseq count (Anders et al., 2013) and filtered for genes on autosomal chromosomes expressed at more than 2 counts per million across all doxorubicin treated samples. The differential expression analysis was performed with EdgeR using generalized linear modeling for biological triplicates with a blocked matrix model for paired comparisons (Robinson et al., 2010). Pathway analysis was performed using GSEA (Subramanian et al., 2005) against c2.all.v4.0.symbol.gmt and enrichment maps (Merico et al., 2010) were made using EnrichmentMapPlugin_v1 in Cytoscape.

ChIP-seq reads were mapped to the UCSC mm9 assembly (Kent et al., 2002) with the Bowtie (ver 0.12.7) short read alignment tool (Langmead et al., 2009) and significant peaks called using the MACS v1.4.2 algorithm (Zhang et al., 2008) using a peak cutoff of $p < 1e-8$. For quantitation of reads in a given region, reads overlapping the region were quantified and considered in the analysis if region counts were < 10 total reads. Metagene analysis was performed with custom R and python scripts.

SUPPLEMENTARY REFERENCES

Anders, S., McCarthy, D. J., Chen, Y., Okoniewski, M., Smyth, G. K., Huber, W., and Robinson, M. D. (2013). Count-based differential expression analysis of RNA sequencing data using R and Bioconductor. *Nat Protoc*, *8*(9), 1765-1786.

Carey, B. W., Markoulaki, S., Hanna, J., Saha, K., Gao, Q., Mitalipova, M., and Jaenisch, R. (2009). Reprogramming of murine and human somatic cells using a single polycistronic vector. *Proc Natl Acad Sci U S A*, *106*(1), 157-162.

Kagey, M. H., Newman, J. J., Bilodeau, S., Zhan, Y., Orlando, D. A., van Berkum, N. L., Ebmeier, C. C., Goossens, J., Rahl, P. B., Levine, S. S., Taatjes, D. J., Dekker, J., and Young, R. A. (2010). Mediator and cohesin connect gene expression and chromatin architecture. *Nature*, *467*(7314), 430-435.

Kent, W. J., Sugnet, C. W., Furey, T. S., Roskin, K. M., Pringle, T. H., Zahler, A. M., and Haussler, D. (2002). The human genome browser at UCSC. *Genome Res*, *12*(6), 996-1006.

Langmead, B., Trapnell, C., Pop, M., and Salzberg, S. L. (2009). Ultrafast and memory-efficient alignment of short DNA sequences to the human genome. *Genome Biol*, *10*(3), R25.

Lewandoski, M., Meyers, E. N., and Martin, G. R. (1997). Analysis of Fgf8 gene function in vertebrate development. *Cold Spring Harb Symp Quant Biol*, *62*, 159-168.

Lowe, S. W., Jacks, T., Housman, D. E., and Ruley, H. E. (1994). Abrogation of oncogene-associated apoptosis allows transformation of p53-deficient cells. *Proc Natl Acad Sci U S A*, *91*(6), 2026-2030.

Merico, D., Isserlin, R., Stueker, O., Emili, A., and Bader, G. D. (2010). Enrichment map: a network-based method for gene-set enrichment visualization and interpretation. *PLoS One*, *5*(11), e13984.

Raj, A., van den Bogaard, P., Rifkin, S. A., van Oudenaarden, A., and Tyagi, S. (2008). Imaging individual mRNA molecules using multiple singly labeled probes. *Nat Methods*, *5*(10), 877-879.

Robinson, M. D., McCarthy, D. J., and Smyth, G. K. (2010). edgeR: a Bioconductor package for differential expression analysis of digital gene expression data. *Bioinformatics*, *26*(1), 139-140.

Rodriguez, C. I., Buchholz, F., Galloway, J., Sequerra, R., Kasper, J., Ayala, R., Stewart, A. F., and Dymecki, S. M. (2000). High-efficiency deleter mice show that FLPe is an alternative to Cre-loxP. *Nat Genet*, *25(2)*(2), 139-140.

Subramanian, A., Tamayo, P., Mootha, V. K., Mukherjee, S., Ebert, B. L., Gillette, M. A., Paulovich, A., Pomeroy, S. L., Golub, T. R., Lander, E. S., and Mesirov, J. P. (2005). Gene set enrichment analysis: a knowledge-based approach for interpreting genome-wide expression profiles. *Proc Natl Acad Sci U S A*, *102*(43), 15545-15550.

Trapnell, C., Pachter, L., and Salzberg, S. L. (2009). TopHat: discovering splice junctions with RNA-Seq. *Bioinformatics*, *25*(9), 1105-1111.

Zhang, Y., Liu, T., Meyer, C. A., Eeckhoute, J., Johnson, D. S., Bernstein, B. E., Nusbaum, C., Myers, R. M., Brown, M., Li, W., and Liu, X. S. (2008). Model-based analysis of ChIP-Seq (MACS). *Genome Biol*, *9*(9), R137.